Anisotropy effects on polar optical phonons in wurtzite GaN/AlN superlattices

J. Gleize, M. A. Renucci, J. Frandon, and F. Demangeot
Laboratoire de Physique des Solides, Université Paul Sabatier, 118 route de Narbonne, 31062 Toulouse cedex 4, France

(Received 11 March 1999; revised manuscript received 15 July 1999)

The dispersion of polar optical phonons in wurtzite AlN/GaN heterostructures grown along the [0001] direction, with particular emphasis on AlN/GaN superlattices, has been calculated within the dielectric continuum model framework. A detailed analysis is given for the interface and confined modes. Features in the dispersion curves are evidenced which are due to the anisotropy of wurtzite crystals. The frequency range for the extraordinary phonons (interface and confined modes) strongly depends on the zone center optical phonon frequencies of bulk GaN and AlN. Moreover, the latter modes are not entirely confined inside one type of layer, but can penetrate inside the surrounding material. Proper confinement of extraordinary phonons can, however, be achieved for zero in-plane wave vector. [S0163-1829(99)10747-1]

I. INTRODUCTION

The group III nitrides GaN and AlN display a promising potential for optoelectronics applications, particularly laser diodes emitting in the blue and ultraviolet frequency range.[1] Although these materials crystallize under ambient conditions in the hexagonal wurtzite structure, few theoretical studies on lattice dynamics and electron-phonon interaction have been devoted so far to wurtzite AlN/GaN heterostructures. The Fröhlich Hamiltonian has been derived in the case of bulk wurtzite crystals[2] and of wurtzite quantum wells (QW's),[3] and the polar optical phonons have also recently been investigated in the latter.[3,4] However, to our knowledge, no such studies have been yet reported on wurtzite AlN/GaN superlattices (SL's).

In contrast, lattice dynamics of SL's have been thoroughly investigated for cubic III–V semiconductors in the last decade. Various macroscopic models have been used to describe the long wavelength phonons in these structures: the hydrodynamic continuum model,[5] with continuous atomic displacements at the interfaces, the dielectric continuum model,[6,7] which fulfills electrostatic boundary conditions, and the more complete continuum model of Chamberlain, Cardona, and Ridley,[8] which takes into account the mixing of confined and interface (IF) modes and lifts the apparent incompatibility of boundary conditions in the two previous models.

The aim of the present work is to analyze the effects of layer anisotropy on polar optical phonons in wurtzite AlN/GaN QW's and SL's. The dielectric model has been chosen in a first approach to the problem, for its simplicity and for its ability to give a physical insight into the phonon picture in quantum well structures. Indeed, although the atomic displacement patterns deduced from electrostatic boundary conditions have not to be considered without caution,[9] this model describes correctly the IF modes dispersion whenever the wave vector dependence of bulk phonon frequencies, as well as mixing with confined modes have not to be considered.[10,11]

Our model is briefly described in Sec. II, along with the main properties of optical polar phonons in bulk wurtzite crystals. Section III is devoted to a GaN QW embedded in AlN, particularly to the existence of proper confined modes in this structure. The study of a wurtzite GaN/AlN SL is performed in Sec. IV and conclusions are given in Sec. V.

II. MODEL

A. Polar modes in a bulk wurtzite crystal

We consider polar optical phonons in wurtzite GaN and AlN, which are uniaxial crystals with space group C_{6v}^4. Due to the anisotropy in these materials, the polar phonon frequencies and the dielectric functions are direction dependent.[12] Taking the z axis along the [0001] direction (**c** axis) and denoting the perpendicular directions as $\perp$, the relationship between the polarization **P** and the relative displacement of the positive and negative sublattices **u(r)** in a bulk wurtzite crystal is given by the equations of motion:[12]

$$\mu \frac{d^2\mathbf{u}_\perp(\mathbf{r})}{dt^2} = -\mu\omega_\perp^2 \mathbf{u}_\perp(\mathbf{r}) + e_\perp^* \mathbf{E}_{loc,\perp}(\mathbf{r}) \tag{1}$$

$$\mu \frac{d^2u_z(\mathbf{r})}{dt^2} = -\mu\omega_z^2 u_z(\mathbf{r}) + e_z^* E_{loc,z}(\mathbf{r}) \tag{2}$$

and

$$\mathbf{P}_\perp(\mathbf{r}) = n e_\perp^* \mathbf{u}_\perp(\mathbf{r}) + n\alpha_\perp \mathbf{E}_{loc,\perp}(\mathbf{r}) \tag{3}$$

$$P_z(\mathbf{r}) = n e_z^* u_z(\mathbf{r}) + n\alpha_z E_{loc,z}(\mathbf{r}) \tag{4}$$

where n is the number of ion pairs per unit volume, μ is the reduced mass of an ion pair, and $\omega_\perp$ and ω_z are the mechanical frequencies, $e_\perp^*$ and e_z^* are the effective charges of the ions, and $\alpha_\perp$ and α_z are the electronic polarizabilities per ion pair, for the $\perp$ and z directions, respectively. The local field $\mathbf{E}_{loc}$ satisfies the Lorentz relationship: $\mathbf{E}_{loc}(\mathbf{r}) = \mathbf{E}(\mathbf{r}) + \mathbf{P}(\mathbf{r})/3\epsilon_0$. The dielectric tensor is given by:

$$\epsilon(\omega)=\begin{pmatrix} \epsilon_\perp(\omega) & 0 & 0 \\ 0 & \epsilon_\perp(\omega) & 0 \\ 0 & 0 & \epsilon_z(\omega) \end{pmatrix} \tag{5}$$

with

$$\epsilon_\perp(\omega)=\epsilon_\perp^\infty\frac{\omega^2-\omega_{\perp,L}^2}{\omega^2-\omega_{\perp,T}^2} \tag{6}$$

and

$$\epsilon_z(\omega)=\epsilon_z^\infty\frac{\omega^2-\omega_{z,L}^2}{\omega^2-\omega_{z,T}^2} \tag{7}$$

where $\epsilon_\perp^\infty$ and ϵ_z^∞ are the optical dielectric constants, $\omega_{\perp,L}$ and $\omega_{z,L}$ are the zone center longitudinal $E_1(LO)$ and $A_1(LO)$ phonon frequencies, $\omega_{\perp,T}$ and $\omega_{z,T}$ are the zone center transverse $E_1(TO)$ and $A_1(TO)$ phonon frequencies of the bulk materials.[12] In the case of GaN and AlN, the anisotropy effect on ϵ^∞ is very weak though, and we shall assume that $\epsilon_\perp^\infty=\epsilon_z^\infty$.[1]

There are three polar optical phonons in a bulk wurtzite crystal:[12] one ordinary wave and two extraordinary waves. The ordinary wave is always transverse and polarized in the $\perp$ plane for any wave vector $\mathbf{q}$. It has E_1 symmetry. The extraordinary waves are associated with z- and $\perp$-polarized vibrations. The z-polarized mode has A_1 symmetry and the $\perp$-polarized one has E_1 symmetry. When the angle θ between $\mathbf{q}$ and $\mathbf{c}$ is 0, one vibration is a $A_1(LO)$ phonon and the other is a $E_1(TO)$ phonon; when θ is varied from 0 to $\pi/2$, these modes gradually become a $A_1(TO)$ and a $E_1(LO)$ phonon, respectively, without having a proper LO or TO character and A_1 or E_1 symmetry. For wurtzite GaN and AlN though, long range Coulomb force effects dominate over the anisotropy in short range interatomic forces. Hence, for $\theta\neq 0,\pi/2$, the extraordinary waves are mixed A_1 and E_1 quasi LO or TO modes.[12,13] The angular dispersion of the extraordinary phonons is given in the long wavelength limit by:[12,14]

$$\epsilon_\perp(\omega)q_\perp^2+\epsilon_z(\omega)q_z^2=0. \tag{8}$$

B. Polar modes in a wurtzite heterostructure: the dielectric continuum model

We now study polar optical phonons in heterostructures composed of wurtzite GaN and AlN. We assume throughout this paper that the heterostructures are grown along the [0001] direction ($\mathbf{c}$ axis) of the bulk materials; we choose the z axis along this direction and denote the perpendicular directions as $\perp$. In order to describe the long wavelength optical phonons dispersion, we use the dielectric continuum model[6] and neglect the effects of retardation, as well as the wave vector dependence of bulk phonon frequencies. We also neglect the lattice mismatch between GaN and AlN. The assumption of fully relaxed layers is obviously unrealistic in physical AlN/GaN systems. As the distribution of strain between the different layers strongly depends on the geometry of the structures and on the nature of the buffer layer, we choose to ignore it first, and then to analyze its consequences on the results we obtained for the extreme situation in which the GaN layers are lattice matched to the fully relaxed AlN layers.

In our calculations, use is made of the fields associated with the polar optical modes rather than of potentials, in order to treat longitudinal and transverse modes at once. In the non-retarded limit, these fields satisfy Maxwell's equations:

$$\nabla\times\mathbf{E}=\mathbf{0} \tag{9}$$

$$\nabla\cdot\mathbf{D}=0 \tag{10}$$

with

$$\mathbf{D}^{(j)}=\epsilon_0\mathbf{E}^{(j)}+\mathbf{P}^{(j)}=\epsilon_0\epsilon_j(\omega)\mathbf{E}^{(j)} \tag{11}$$

and

$$\mathbf{P}^{(j)}=\epsilon_0\chi_j(\omega)\mathbf{E}^{(j)} \tag{12}$$

where j specifies the nature of the layer ($j=1$ for GaN and $j=2$ for AlN).

The translational invariance being conserved in the $\perp$ plane, we can use a 2-D Fourier transform in this plane.[6] With a suitable choice for the basis in $\mathbf{q}_\perp$ space, we have $\mathbf{q}_\perp=(q_\perp,0)$ and Eq. (9) yields:

$$\frac{d}{dz}E_x^{(j)}(z)-iq_\perp E_z^{(j)}(z)=0 \tag{13}$$

and

$$\frac{d}{dz}E_y^{(j)}(z)=0 \quad\text{and}\quad iq_\perp E_y^{(j)}(z)=0. \tag{14}$$

The polarization is thus separated into an s-polarized part $\mathbf{P_s}=(0,P_s=P_y,0)$, corresponding to the ordinary phonon, and a p-polarized part $\mathbf{P_p}=(P_\perp=P_x,0,P_z)$, corresponding to the extraordinary phonons, which are completely decoupled and satisfy:

$$\frac{d}{dz}[\chi_{\perp,j}^{-1}(\omega)P_s^{(j)}(z)]=0 \tag{15}$$

and

$$iq_\perp\chi_{\perp,j}^{-1}(\omega)P_s^{(j)}(z)=0 \tag{16}$$

for the s-polarized part, and

$$\chi_{\perp,j}^{-1}(\omega)\frac{dP_\perp^{(j)}(z)}{dz}-iq_\perp\chi_{z,j}^{-1}(\omega)P_z^{(j)}(z)=0 \tag{17}$$

for the p-polarized part. Furthermore, Eq. (10) gives:

$$iq_\perp\frac{\epsilon_{\perp,j}(\omega)}{\chi_{\perp,j}(\omega)}P_\perp^{(j)}(z)+\frac{\epsilon_{z,j}(\omega)}{\chi_{z,j}(\omega)}\frac{dP_z^{(j)}(z)}{dz}=0. \tag{18}$$

From Eqs. (17) and (18), we deduce that the z and $\perp$ components of $\mathbf{P_p}$ are described by functions which have opposite parity with respect to the $z=0$ plane. We shall consider throughout this paper the symmetry of vector $\mathbf{P_p}$. In the case of a QW, for instance, we shall call symmetric (S) all modes for which the $z=0$ plane is a symmetry plane for $\mathbf{P_p}$ (i.e. for

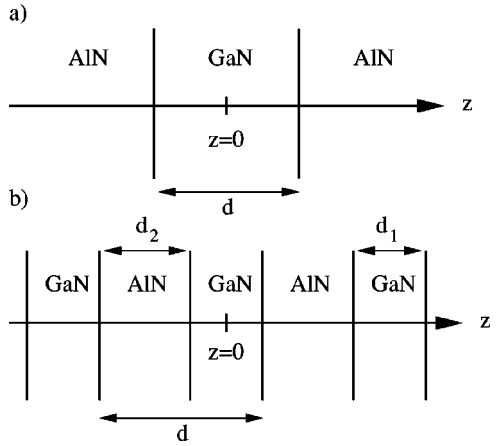

FIG. 1. Description of the two wurtzite heterostructures studied in this paper: (a) a GaN QW of width d embedded in infinite AlN barriers and (b) an infinite GaN/AlN SL; the widths of the GaN and AlN layers are d_1 and d_2, respectively, and $d=d_1+d_2$ is the period of the SL. In both cases, the growth direction (z axis) is parallel to the **c** axis of wurtzite GaN and AlN.

even $P_\perp$ and odd P_z), and antisymmetric (AS) all modes for which the $z=0$ plane is an anti-symmetry plane for $\mathbf{P_p}$ (i.e. for odd $P_\perp$ and even P_z).

Solving Eqs. (15)–(18), with electrostatic boundary conditions at each interface, namely

$$\chi_{\perp,1}^{-1}(\omega)P_\perp^{(1)}(z)]_{int.}=\chi_{\perp,2}^{-1}(\omega)P_\perp^{(2)}(z)]_{int.} \tag{19}$$

for the continuity of $E_\perp$, and

$$\left.\frac{\epsilon_{z,1}(\omega)}{\chi_{z,1}(\omega)}P_z^{(1)}(z)\right]_{int.}=\left.\frac{\epsilon_{z,2}(\omega)}{\chi_{z,2}(\omega)}P_z^{(2)}(z)\right]_{int.} \tag{20}$$

for the continuity of D_z, we can obtain the dispersion relationships for the polar optical modes.

III. POLAR OPTICAL PHONONS IN A WURTZITE (AlN/GaN/AlN) QUANTUM WELL

We consider a wurtzite GaN QW of width d, as described in Fig. 1(a). The z axis origin is taken at the center of the QW. A recent theoretical study of this system[3,4] classified its polar optical phonons into four distinct types of modes: interface modes (IF), quasi-confined modes (QC), half space modes (HS), and propagating modes (PR). As we are mainly interested in the comparison of the polar modes dispersion of a QW to that of a SL, we ignore the HS modes, as they cannot be observed in an infinite SL, and the PR modes, because they do not appear in an unstrained wurtzite GaN/AlN heterostructure.[3] On the other hand, we shall briefly present the IF and QC modes dispersion, and focus our attention on the existence of proper confined modes in a wurtzite QW, which was ruled out in Ref. 3 and Ref. 4. Indeed, the authors restrict their analysis to guided modes with $q_\perp\neq 0$, since the continuity of the scalar potential they used is implicitely taken as equivalent to that of $E_\perp$.

We examine the p-polarized $\omega\neq\omega_{z,L}^j$ and $\omega\neq\omega_{\perp,T}^j$ solutions; Eqs. (17) and (18) yield:

$$\frac{d^2}{dz^2}P_\perp^{(j)}(z)+q_{z,j}^2(\omega)P_\perp^{(j)}(z)=0 \tag{21}$$

where $q_{z,j}(\omega)$ is given by the angular dispersion of the bulk constituents (8). The p-polarization then takes the general form:

$$P_\perp^{(j)}=A_j e^{iq_{z,j}(\omega)z}+B_j e^{-iq_{z,j}(\omega)z} \tag{22}$$

when z belongs to a j layer. In this paper, we only consider modes that cannot propagate through the barriers, hence we can set $\epsilon_{\perp,2}(\omega)/\epsilon_{z,2}(\omega)\geqslant 0$ without loss of generality. Moreover, the fields in the barriers must vanish when $z\rightarrow\pm\infty$. With these new boundary conditions and with Eqs. (19) and (20) at the $z=\pm d/2$ interfaces, we obtain the secular equation:

$$[-a_1(\omega)\sin(q_{z,1}(\omega)d/2)+a_2(\omega)\cos(q_{z,1}(\omega)d/2)]\times[a_1(\omega)\cos(q_{z,1}(\omega)d/2)+a_2(\omega)\sin(q_{z,1}(\omega)d/2)]=0 \tag{23}$$

where

$$a_1(\omega)=\epsilon_{z,1}(\omega)q_{z,1}(\omega)/q_\perp$$

and

$$a_2(\omega)=\mathrm{sign}[\epsilon_{z,2}(\omega)]\sqrt{\epsilon_{z,2}(\omega)\epsilon_{\perp,2}(\omega)}.$$

A. Interface modes and quasi-confined modes

IF modes may appear when $q_z(\omega)$ is imaginary for both the well and barriers,[4,7] i.e. when $\epsilon_{\perp,j}(\omega)/\epsilon_{z,j}(\omega)\geqslant 0$ for both GaN and AlN. Thus, the waves cannot propagate through the structure along z and the associated fields decay exponentially away from the interfaces. In addition, we must have $\epsilon_{z,1}(\omega)\epsilon_{z,2}(\omega)\leqslant 0$ for the IF modes to exist. All these conditions imply that the existence of IF modes strongly depends on the relative values of the zone center phonon frequencies of the bulk constituents, which is not the case for cubic materials. These modes are not purely LO or TO modes, as $\mathbf{P_p}$ has a non zero z component. Setting $\gamma_1(\omega)=q_\perp\sqrt{\epsilon_{\perp,1}(\omega)/\epsilon_{z,1}(\omega)}$ and $a_1(\omega)=\mathrm{sign}[\epsilon_{z,1}(\omega)]\sqrt{\epsilon_{z,1}(\omega)\epsilon_{\perp,1}(\omega)}$, their dispersion relationships are given by:

$$a_1(\omega)\cosh(\gamma_1(\omega)d/2)+a_2(\omega)\sinh(\gamma_1(\omega)d/2)=0 \tag{24}$$

for the AS modes and

$$a_1(\omega)\sinh(\gamma_1(\omega)d/2)+a_2(\omega)\cosh(\gamma_1(\omega)d/2)=0 \tag{25}$$

for the S modes.

QC modes appear when $q_{z,j}$ is real for the well and imaginary for the barriers.[3,4] They display an interface behavior in the barriers and a confined behavior in the well; this situation is very similar to that of electrons confined in a QW of finite depth.[15] The confinement in the QW leads to a quantization of $q_{z,1}$ characterized by an integer m which defines the order

of the corresponding QC modes. Setting $b_1(\omega) = \mathrm{sign}[\epsilon_{z,1}(\omega)]\sqrt{|\epsilon_{z,1}(\omega)\epsilon_{\perp,1}(\omega)|}$, the QC modes dispersion relationships are given by:

$$b_1(\omega)\cos(q_{z,1}^m(\omega)d/2)+a_2(\omega)\sin(q_{z,1}^m(\omega)d/2)=0 \quad (26)$$

for the AS modes, with $2m\pi/d<q_{z,1}^m<(2m+1)\pi/d$, where $m=0,1,2,\ldots$,[16] and

$$a_2(\omega)\cos(q_{z,1}^m(\omega)d/2)-b_1(\omega)\sin(q_{z,1}^m(\omega)d/2)=0 \quad (27)$$

for the S modes, with $(2m+1)\pi/d<q_{z,1}^m<2(m+1)\pi/d$, where $m=0,1,2,\ldots$.[16]

B. Confined modes

We now consider the existence of proper confined modes in a wurtzite QW. Clearly, as pointed out by Komirenko *et al.*,[4] all $q_\perp\neq 0$ modes cannot be properly confined due to the anisotropy of wurtzite materials. The situation is different, however, when $q_\perp=0$. Equation (21) is not valid anymore, so we must use Eqs. (17) and (18) and the boundary conditions (19) and (20). We shall focus our attention on the frequencies of interest at $q_\perp=0$, namely the GaN A_1(LO) and E_1(LO) frequencies. Setting $\mathbf{P_p}^{(2)}=\mathbf{0}$ and $q_\perp=0$, we obtain the boundary conditions:

$$\chi_{\perp,1}^{-1}(\omega)P_\perp^{(1)}(z)\big|_{z=\pm d/2}=0 \quad (28)$$

and

$$\chi_{z,1}^{-1}(\omega)\epsilon_{z,1}(\omega)P_z^{(1)}(z)\big|_{z=\pm d/2}=0 \quad (29)$$

Furthermore, inside the well, Eqs. (17) and (18) become:

$$\chi_{\perp,1}^{-1}(\omega)\frac{d}{dz}P_\perp^{(1)}(z)=0 \quad (30)$$

and

$$\chi_{z,1}^{-1}(\omega)\epsilon_{z,1}(\omega)\frac{d}{dz}P_z^{(1)}(z)=0 \quad (31)$$

as $\chi_{z,1}^{-1}(\omega)\neq 0,\infty$ and $\chi_{\perp,1}^{-1}(\omega)\epsilon_{\perp,1}(\omega)\neq 0,\infty$ for the frequencies of interest.

When $\omega=\omega_{z,L}^{(1)}$, $\epsilon_{z,1}(\omega)=0$ and $\chi_{\perp,1}^{-1}(\omega)$ and $\chi_{z,1}^{-1}(\omega)\neq 0,\infty$. Equations (29) and (31) are then satisfied for any $P_{z,1}$ and Eq. (30) gives $dP_{\perp,1}/dz=0$. With the boundary condition (28), we obtain $P_{\perp,1}=0$. Confined A_1(LO) phonons can therefore exist in the GaN well for $q_\perp=0$. As in the case of a cubic heterostructure,[17,18] the confinement leads to a quantization of their phonon wave vector $q_{z,1}$ whose values can be derived from the dispersion relationships of the QC modes in the limit $\omega\to\omega_{z,L}^1$: $q_{z,1}^m=(2m+1)\pi/d$ for the S modes, where $m=0,1,2,\ldots$ and $q_{z,1}^m=2m\pi/d$ for the AS modes, where $m=0,1,2,\ldots$.

We now examine the $\omega=\omega_{\perp,T}^{(1)}$ solution, i.e. $\chi_{\perp,1}^{-1}(\omega)=0$ and $\chi_{z,1}^{-1}(\omega)\epsilon_{z,1}(\omega)\neq 0,\infty$. In this case, Eqs. (30) and (28) are satisfied for any $P_{\perp,1}$ and Eq. (31) gives $dP_{z,1}/dz=0$. With the boundary condition (29), we obtain $P_{z,1}=0$. Confined E_1 (TO) phonons can therefore exist in the GaN well with $q_\perp=0$. Their wave vector $q_{z,1}$ is also quantized and its values can be obtained from the dispersion relationships of the QC modes in the limit $\omega\to\omega_{\perp,T}^1$: $q_{z,1}=2(m+1)\pi/d$ for the S modes, where $m=0,1,2,\ldots$, and $q_{z,1}=(2m+1)\pi/d$ for the AS modes, where $m=0,1,2,\ldots$.

The $\omega=\omega_{z,T}^1$ and $\omega=\omega_{\perp,L}^1$ cases only lead to trivial solutions, hence no confined A_1(TO) or E_1(LO) modes are allowed in a wurtzite heterostructure grown along the [0001] direction.

We have thus demonstrated the existence of confined modes in a wurtzite QW, which appear to be the $q_\perp=0$ limit of the QC modes. However, the values we obtained for the quantized $q_{z,1}$ lead to a discontinuous ionic displacement $\mathbf{u}$ at the interfaces. This is one of the major drawbacks of the dielectric continuum model which uses electrostatic boundary conditions.[19] We must note that in the particular $q_\perp=0$ case though, these conditions are satisfied for any $\mathbf{P_p}^{(1)}$. $P_\perp^{(1)}(z)$ and $P_z^{(1)}(z)$ are then arbitrary functions. So, additional matching boundary conditions achieving the continuity of atomic displacements at the interfaces could be adopted. This was done by Jusserand and Cardona[20] in the case of cubic heterostructures, in order to recover the same symmetry patterns as predicted by microscopic models (see also Ref. 23). This choice, however, would give values of $q_{z,1}$ which could not be related to the $q_\perp\to 0$ limit of the QC mode dispersion.

We consider finally the s-polarized solutions. Equations (15) and (16) with the boundary conditions at $z=\pm d/2$ yield $\omega=\omega_{\perp,T}^1$ and $\mathbf{P_s}=\mathbf{0}$ in the barriers for any $q_\perp$. We thus have confined ordinary E_1 (TO) phonons in the GaN well which are not dispersive. As in the case of the $q_\perp=0$ p-polarized modes, the electrostatic boundary conditions are satisfied for any $\mathbf{P_s}^{(1)}$, but they are also satisfied for any $q_\perp$. So, we can choose boundary conditions which yield zero displacement at the interfaces. The values of the quantized $q_{z,1}$ wave vector are then $q_{z,1}=(2m+1)\pi/d$ for the S modes and $q_{z,1}=2(m+1)\pi/d$ for the AS modes, with $m=0,1,2,\ldots$.

C. Comments

The dispersion curves for a wurtzite GaN QW embedded in infinite AlN barriers are given in Fig. 2. We used in our calculations the zone-center frequencies for unstrained GaN and AlN which are listed in Table I.

Since the A_1-E_1 splitting domains of unstrained AlN and GaN do not overlap, the $\epsilon_{z,1}(\omega)\epsilon_{z,2}(\omega)\leqslant 0$ condition for the existence of IF modes is fulfilled for two distinct frequency ranges. Thus, four IF phonon branches are obtained, as in the case of a cubic QW. Two IF branches (S and AS) belong to the LO range, between the GaN E_1(LO) and the AlN A_1(LO) frequencies, and the two others (S and AS) are found in the TO range, between the GaN E_1(TO) and the AlN A_1(TO) frequencies. In the limit $q_\perp d\gg 1$, the S and AS modes of each region become degenerate and correspond to decoupled vibrations which are strongly localized at the QW interfaces. A striking consequence of the anisotropy of the bulk constituents of the wurtzite QW is that the AS IF branch lying in the LO range reaches the GaN E_1 (LO) frequency, for which $q_{z,1}=0$, for a non zero $q_\perp$. Consequently, for very small $q_\perp$, $q_{z,1}$ becomes real and this branch corresponds to AS QC phonons with $m=0$ (see insert in Fig. 2).

As far as the QC modes are concerned, we note that $q_{z,1}$ is defined using Eq. (8), which gives the angular dispersion of bulk GaN. Hence, their dispersion is similar to the angular

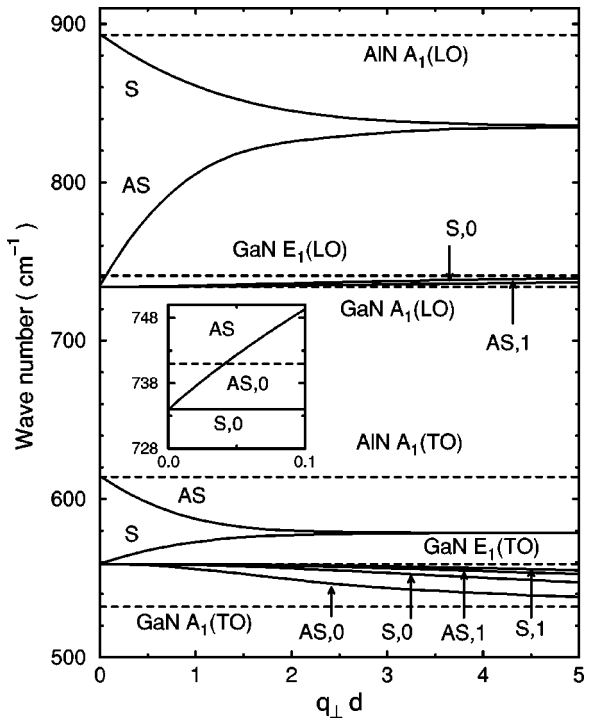

FIG. 2. IF and QC mode dispersion curves for a GaN QW embedded in infinitely wide AlN barriers. Both the well and the barriers are supposed to be unstrained. The modes are symmetric (S) or antisymmetric (AS) with respect to the middle plane of the GaN layer. In the case of QC modes, the value of their order *m* is also displayed.

dispersion of the polar modes in this material.[14] The QC branches are found in the LO domain, between the GaN $A_1(LO)$ and $E_1(LO)$ frequencies, and in the TO domain, between the GaN $A_1(TO)$ and $E_1(TO)$ frequencies. They are more dispersive for decreasing *m* (i.e. for decreasing $q_{z,1}$). For $q_\perp = 0$, the vibrations (at the $A_1(LO)$ and $E_1(TO)$ frequencies) are totally confined in the QW and for non zero $q_\perp$, they can penetrate in the barriers. For large $q_\perp$, the LO and TO QC branches approach the $E_1(LO)$ and $A_1(TO)$ frequencies, respectively, as would be the case in bulk GaN for an angle θ between **c** and **q** approaching the value $\pi/2$. Nevertheless, such values could not be reached, for example, in a Raman experiment where $q_\perp^{max} = 4\pi\langle n\rangle/\lambda$ ($\langle n\rangle$ is the mean refractive index of the structure). Indeed, for λ in the visible-UV domain and a QW of 10 monolayers width, $q_\perp^{max} d$ is typically in the 0.1–0.3 range.

Although our calculations were performed for unstrained materials, the results we obtained still give a qualitative insight into the polar phonon dispersion of a more realistic system, where the GaN QW is lattice matched to the infinite AlN barriers. In this case, due to the 2.4% lattice mismatch between GaN and AlN, the GaN QW experiences a compressive strain and the zone center phonon frequencies of GaN are shifted to higher values. Using the deformation potentials measured for biaxially strained wurtzite GaN, we calculated the shifts of the $A_1(TO)$ and $E_1(TO)$ modes,[21] and of the $A_1(LO)$ phonon.[22] The values we obtained are 16 cm^{-1}, 32 cm^{-1}, and 9 cm^{-1}, respectively. On the other hand, the intervals which separate the unstrained AlN and GaN phonon frequencies are 152 cm^{-1} and 55 cm^{-1} in the LO and TO range, respectively. Hence, although the IF domains are reduced, particularly in the TO range, the relative position of the GaN zone center phonon frequencies with respect to those of AlN remain unchanged and our general comments on the polar phonon dispersion in a GaN QW are still valid.

TABLE I. Zone center frequencies (in cm^{-1}) of polar optical phonons and optical dielectric constants of wurtzite GaN and AlN.

Material	$A_1(TO)$	$E_1(TO)$	$A_1(LO)$	$E_1(LO)$	ϵ^{∞} [a]
GaN[b]	532	559	734	741	5.35
AlN[c]	614	673	893	916	4.84

[a]The values for ϵ^{∞} are taken from Ref. 1.
[b]Reference 25.
[c]Reference 26.

IV. POLAR OPTICAL PHONONS IN A WURTZITE (AlN/GaN) SUPERLATTICE

We shall now study the polar optical modes in an infinite wurtzite (GaN/AlN) SL as described in Fig. 1(b). The GaN and AlN layers have d_1 and d_2 width, respectively and the period of the SL is $d = d_1 + d_2$. Due to the periodic stacking of layers in the [0001] direction, we can use Bloch's theorem and express the electric field in the n^{th} period as: $\mathbf{E}(z) = \mathbf{E}(z - nd)e^{iQ_z nd}$, where Q_z belongs to the first Brillouin zone of the SL: $-\pi/d \leqslant Q_z \leqslant +\pi/d$. In this case, we only need to take into account the boundary conditions at the $z = \pm d_1/2$ interfaces, which, using Eq. (21), yield the secular equation:

$$\cos(Q_z d) = \cos(q_{z,1}(\omega) d_1/2)\cos(q_{z,2}(\omega) d_2/2) - \left[\frac{a_1(\omega)}{a_2(\omega)} + \frac{a_2(\omega)}{a_1(\omega)}\right]\sin(q_{z,1}(\omega) d_1/2) \times \sin(q_{z,2}(\omega) d_2/2) \quad (32)$$

with $a_j(\omega) = \epsilon_{z,j}(\omega) q_{z,j}(\omega)/q_\perp$. This equation gives the dispersion relationship of the polar modes in an infinite wurtzite SL. Due to the periodicity in this system, the $Q_z = 0$ modes have the same symmetry with respect to the middle plane of *any* layer (GaN or AlN), whereas the $Q_z = \pi/d$ modes have opposite symmetries with respect to the middle planes of the AlN and GaN layers. In the following subsections, we shall denote as $S^{(j)}$ and $AS^{(j)}$ the modes which are symmetric and antisymmetric with respect to the middle plane of *any j* layer, respectively.

A. Interface modes

Interface phonons appear when $\epsilon_{\perp,j}(\omega)/\epsilon_{z,j}(\omega) \geqslant 0$ for both GaN and AlN and $\epsilon_{z,1}(\omega)\epsilon_{z,2}(\omega) \leqslant 0$, as already discussed in Sec. III. The dispersion relationship (32) can be simplified for the values $Q_z = 0$ and π/d; setting $a_j(\omega) = \mathrm{sign}[\epsilon_{z,j}(\omega)]\sqrt{\epsilon_{z,j}(\omega)\epsilon_{\perp,j}(\omega)}$ and

$$\gamma_j(\omega) = q_\perp \sqrt{\epsilon_{\perp,j}(\omega)/\epsilon_{z,j}(\omega)},$$

we obtain:

$$a_1(\omega)\coth(\gamma_1(\omega)d_1/2)+a_2(\omega)\coth(\gamma_2(\omega)d_2/2)=0 \tag{33}$$

for the $Q_z=0$ $AS^{(1)}$ and $AS^{(2)}$ modes,

$$a_1(\omega)\coth(\gamma_1(\omega)d_1/2)+a_2(\omega)\tanh(\gamma_2(\omega)d_2/2)=0 \tag{34}$$

for the $Q_z=\pi/d$ $AS^{(1)}$ and $S^{(2)}$ modes,

$$a_1(\omega)\tanh(\gamma_1(\omega)d_1/2)+a_2(\omega)\tanh(\gamma_2(\omega)d_2/2)=0 \tag{35}$$

for the $Q_z=0$ $S^{(1)}$ and $S^{(2)}$ modes, and

$$a_1(\omega)\tanh(\gamma_1(\omega)d_1/2)+a_2(\omega)\coth(\gamma_2(\omega)d_2/2)=0 \tag{36}$$

for the $Q_z=\pi/d$ $S^{(1)}$ and $AS^{(2)}$ modes.

B. Quasi-confined and confined modes

QC phonons appear when $\epsilon_\perp(\omega)/\epsilon_z(\omega)\leqslant 0$ for either GaN or AlN. They display a confined behavior in layers denoted as j and an interface character in layers denoted as l. The confinement in the j layers leads to a quantization of $q_{z,j}$, which we shall label by an integer m. Setting $a_l(\omega)=\text{sign}[\epsilon_{z,l}(\omega)]\sqrt{\epsilon_{z,l}(\omega)\epsilon_{\perp,l}(\omega)}$,

$$b_j(\omega)=\text{sign}[\epsilon_{z,j}(\omega)]\sqrt{|\epsilon_{z,j}(\omega)\epsilon_{\perp,j}(\omega)|},$$

and

$$\gamma_l(\omega)=q_\perp\sqrt{\epsilon_{\perp,l}(\omega)/\epsilon_{z,l}(\omega)},$$

the QC modes dispersion relationships can be expressed as:

$$b_j(\omega)\cot(q^m_{z,j}(\omega)d_j/2)+a_l(\omega)\coth(\gamma_l(\omega)d_l/2)=0 \tag{37}$$

for the $Q_z=0$ $AS^{(j)}$ modes and

$$b_j(\omega)\cot(q^m_{z,j}(\omega)d_j/2)+a_l(\omega)\tanh(\gamma_l(\omega)d_l/2)=0 \tag{38}$$

for the $Q_z=\pi/d$ $AS^{(j)}$ modes, with the condition $2m\pi/d_j<q^m_{z,j}<(2m+1)\pi/d_j$ if $\epsilon_{z,1}(\omega)\epsilon_{z,2}(\omega)<0$ and $(2m+1)\pi/d_j<q^m_{z,j}<2(m+1)\pi/d_j$ if $\epsilon_{z,1}(\omega)\epsilon_{z,2}(\omega)>0$ where $m=0,1,2,\ldots$, and:

$$b_j(\omega)\tan(q^m_{z,j}(\omega)d_j/2)-a_l(\omega)\tanh(\gamma_l(\omega)d_l/2)=0 \tag{39}$$

for the $Q_z=0$ $S^{(j)}$ modes and

$$b_j(\omega)\tan(q^m_{z,j}(\omega)d_j/2)-a_l(\omega)\coth(\gamma_l(\omega)d_l/2)=0 \tag{40}$$

for the $Q_z=\pi/d$ $S^{(j)}$ modes, with the condition $2m\pi/d_j<q^m_{z,j}<(2m+1)\pi/d_j$ if $\epsilon_{z,1}(\omega)\epsilon_{z,2}(\omega)>0$ and $(2m+1)\pi/d_j<q^m_{z,j}<2(m+1)\pi/d_j$ if $\epsilon_{z,1}(\omega)\epsilon_{z,2}(\omega)<0$ where $m=0,1,2,\ldots$

Proper confined modes can also appear in a wurtzite GaN/AlN SL. Following the procedure described in Sec. III B, we obtain confined p-polarized phonons at the AlN (if $j=2$) and GaN (if $j=1$) A_1(LO) and E_1(TO) frequencies for $q_\perp=0$ and s-polarized phonons at the AlN (if $j=2$) and GaN (if $j=1$) E_1(TO) frequency for any $q_\perp$. The derivation of the corresponding quantized wave vectors $q_{z,j}$ is then performed as in Sec. III B, raising a similar problem concerning the validity of electrostatic boundary conditions.

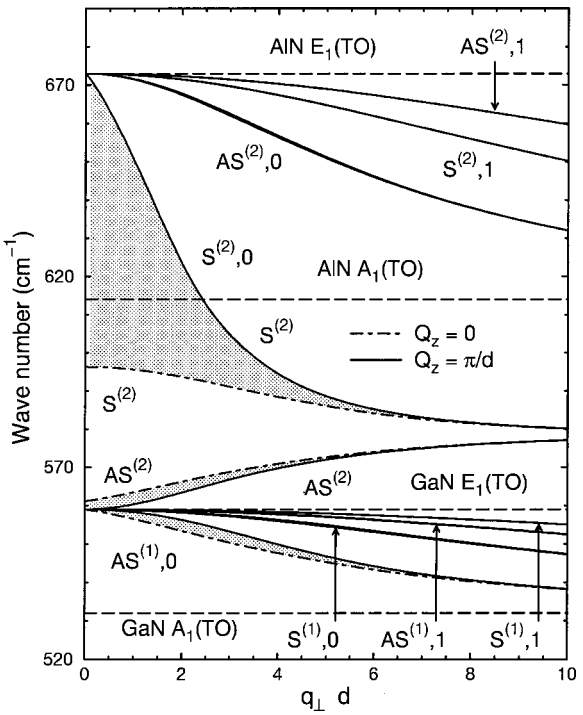

FIG. 3. Dispersion of IF and QC modes for an infinite and unstrained AlN(5 nm)/GaN(5 nm) SL in the TO frequency range. The shaded areas are bands which correspond to all the values of Q_z lying in the first Brillouin zone of the SL. The symmetry of the modes is given with respect to the middle planes of the j layers, where $j=1$ for GaN and $j=2$ for AlN. The QC modes are identified by their order m.

C. Discussion

The IF and QC dispersion curves for an infinite and unstrained 5 nm AlN / 5 nm GaN SL are given in Figs. 3 and 4 for the TO and LO frequency range, respectively. We have used in our calculations the GaN and AlN parameters listed in Table I. We obtain series of branches (one for each value of Q_z lying in the first Brillouin zone of the SL) which form bands.

As already discussed in Sec. III, four IF modes bands are found. Two IF bands belong to the LO region between the GaN E_1(LO) and the AlN A_1(LO) frequencies, and the two others lie in the TO region between the GaN E_1(TO) and the AlN A_1(TO) frequencies. The two IF bands found in the LO or TO domain become degenerate for large $q_\perp$, which corresponds to independent vibrations strongly localized at the SL's interfaces. As in the case of cubic materials, the symmetry of the $Q_z=0$ branches depends on the d_1/d_2 ratio.[20,23] For $d_1=d_2$, the $Q_z=0$ and $Q_z=\pi/d$ branches limiting a same band have the same symmetry with respect to the middle plane of layers 1 and 2 in the LO and TO domains, respectively (S for the upper band and AS for the lower one). However, although $d_1=d_2$, the $Q_z=0$ branches are not degenerate, as they would be in a cubic SL.[20,23] Indeed, due to the anisotropy of the wurtzite layers, the energy gap between the upper and lower $Q_z=0$ branches disappears for different values of d_2/d_1 in the TO and LO regions

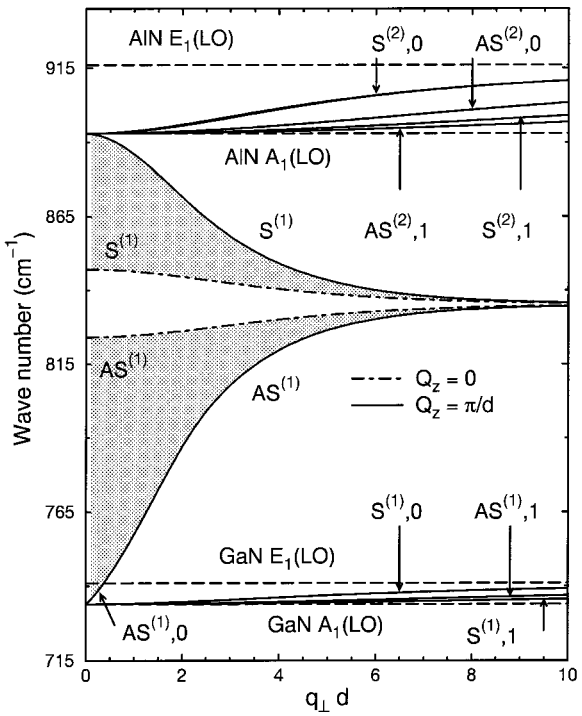

FIG. 4. Dispersion of IF and QC modes for an infinite and unstrained AlN(5 nm)/GaN(5 nm) SL in the LO frequency range. The symmetry of the modes is given with respect to the middle planes of the j layers, where $j=1$ for GaN and $j=2$ for AlN. The QC modes are identified by their order m.

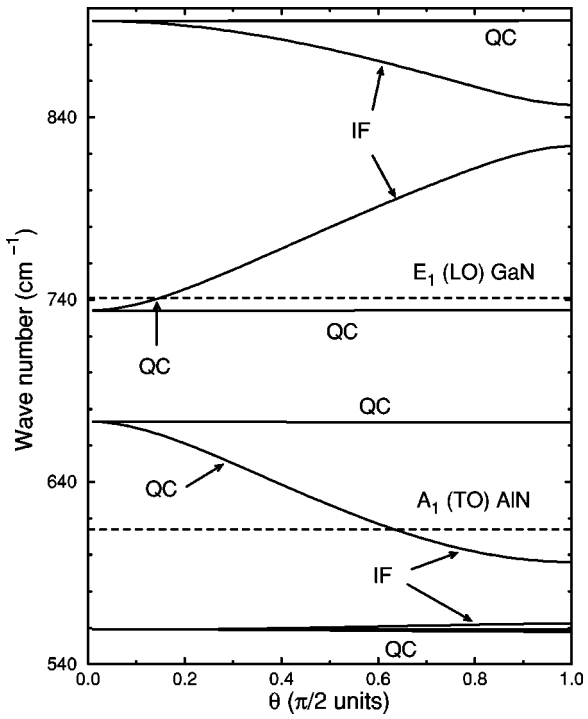

FIG. 5. Angular dispersion of the polar optical modes (IF and QC modes) in the wurtzite GaN/AlN SL. These curves are deduced from the results displayed in Fig. 3 and Fig. 4 for $qd=0.6$. All QC modes show a very weak dispersion with the exception of the $m=0$ $AS^{(1)}$ modes.

($d_2/d_1 \approx 2.50$ and $d_2/d_1 \approx 0.74$, respectively). Consequently, the dependence on the layers widths of the symmetry of the $Q_z=0$ IF mode branches is different for the LO and TO ranges.

QC modes are found in the E_1-A_1 splitting regions of GaN and AlN. Indeed, the finite width of the AlN layers turns the half space modes, which are obtained for a GaN/AlN QW in the AlN E_1-A_1 splitting domain,[3,4] into modes which are quasi-confined inside the AlN layers. As pointed out in Sec. III, these QC branches display a dispersion which is similar to that of the polar optical phonons of bulk GaN and AlN. Generally speaking, the QC mode bands are very narrow: the dispersion curves do not appear to depend on Q_z, with the exception of the $AS^{(1)}$ $m=0$ GaN QC band found in the TO region. More important, the AlN A_1(TO) frequency, for which $q_{z,2}=0$, is now reached for a non zero $q_\perp$. This is essentially due to the finite thickness of the AlN layers which introduces $q_{z,2}(\omega)$ dependent terms in the IF and QC phonons dispersion relationships. Thus, the same feature which was observed in the case of a GaN QW at the GaN E_1(LO) frequency appears in an AlN/GaN SL at the AlN A_1(TO) frequency. The corresponding $Q_z=\pi/d$ branches extend in a frequency range which includes an IF and a QC region and the associated modes are QC phonons for small $q_\perp d$ and IF phonons for larger $q_\perp d$. In addition, we must note that the symmetry of these particular $Q_z=\pi/d$ branches is conserved as they evolve from a QC to an IF behavior.

The periodic stacking of layers in the z direction does not alter the hexagonal symmetry. Thus, all polar modes show an angular dispersion which depends on the value of q. Figure 5 shows the calculated angular dispersion for $qd=0.6$, as a function of the angle θ between the **c** axis and the phonon wave vector **q**. This value can be obtained in a backscattering Raman experiment, for example, where q is typically $q=4\pi\langle n\rangle d/\lambda$, for $\lambda=488$ nm. The curves corresponding to most QC modes are almost flat. This is due to the narrowness of the corresponding bands shown in Fig. 3 and Fig. 4, and to the small value of qd. On the contrary, the IF modes show a stronger angular dispersion, particularly the two branches which are partly QC and partly IF. These are confined modes for $\theta=0$ (i.e., $q_\perp=0$) and IF modes for $\theta=\pi/2$ (i.e., $Q_z=0$). When the angle θ is varied from 0 to $\pi/2$, they gradually lose their confined character and become IF modes.

Our calculations were performed under the assumption that both GaN and AlN were unstrained, which is not true in real SLs.[24] As no data are currently available concerning the deformation potentials of wurtzite AlN, further work is needed to obtain reliable theoretical dispersion curves for the polar optical phonons in wurtzite AlN/GaN heterostructures. However, in the case where the GaN layers are lattice matched to the AlN layers, the frequency shifts of the zone center phonons of GaN can be estimated.[21,22] As pointed out in Sec. III, the TO range IF domain is then drastically reduced and the corresponding IF bands should become very narrow and display very little angular dispersion. In addition, the TO range GaN QC region is enlarged, and the $m=0$ GaN QC band should become wider and display a stronger angular dispersion than for unstrained materials. On the contrary, the LO range bands should hardly be changed by strain effects in the GaN layers, as the IF modes domain is still much larger than the QC modes region.

V. CONCLUSIONS

We have calculated the dispersion of the polar optical phonons in wurtzite AlN/GaN heterostructures grown along the [0001] direction within the dielectric continuum framework. Features appear in the dispersion curves, due to the anisotropy of the bulk constituents.

Our calculations, however, neglect the lattice mismatch which exists between wurtzite GaN and AlN (about 2.4%). In a real SL, the GaN and AlN layers are strained and the bulk zone center frequencies used as input data are no longer valid. On the other hand, the following features in the dispersion of the polar phonons in wurtzite SLs, which are only due to the anisotropy of the layers, are still valid.

The existence of IF modes strongly depends on the relative values of the zone center frequencies of GaN and AlN and the confined modes branches become dispersive. Moreover, proper confinement of the extraordinary phonons inside one type of layer can only be achieved for zero in-plane wave vector $q_\perp$. When $q_\perp \neq 0$, the polarization associated with the polar optical modes can penetrate in the surrounding layers, where they decay exponentially, and these modes are quasi-confined. The most striking feature due to the anisotropy of GaN and AlN is the change of mode type from QC to IF which occurs when the dispersion curves reach the GaN E_1(LO) frequency (and the AlN A_1(TO) frequency in the case of a SL) for non zero $q_\perp$.

For a SL, the dispersion curves form bands which are narrower for higher order QC modes. Consequently, the angular dispersion of these modes is very weak compared to that of the IF modes. The symmetry of the QC and IF modes depends on the layers widths d_1 and d_2 and an energy gap is observed between IF branches of opposite symmetry in the LO and TO ranges, even for $d_1 = d_2$.

ACKNOWLEDGMENT

ESA 5477 associée au CNRS.

[1] H. Morkoc, S. Strite, G. B. Gao, M. E. Lin, B. Sverdlov, and M. Burns, J. Appl. Phys. **76**, 1363 (1994).
[2] B. C. Lee, K. W. Kim, M. A. Stroscio, and M. Dutta, Phys. Rev. B **56**, 997 (1997).
[3] B. C. Lee, K. W. Kim, M. A. Stroscio, and M. Dutta, Phys. Rev. B **58**, 4860 (1998).
[4] S. M. Komirenko, K. W. Kim, M. Dutta, and M. A. Stroscio, Phys. Rev. B **59**, 5013 (1999).
[5] M. Babiker, J. Phys. C **19**, 683 (1986).
[6] L. Wendler, Phys. Status Solidi B **129**, 513 (1985).
[7] R. E. Camley and D. L. Mills, Phys. Rev. B **29**, 1695 (1984).
[8] M. P. Chamberlain, M. Cardona, and B. K. Ridley, Phys. Rev. B **48**, 14 356 (1993).
[9] C. Trallero-Giner, F. Garcia-Moliner, V. R. Velasco, and M. Cardona, Phys. Rev. B **45**, 11 944 (1992).
[10] B. Zhu, Phys. Rev. B **38**, 7694 (1988).
[11] R. Hessmer, A. Huber, T. Egeler, M. Haines, G. Tränkle, G. Weimann, and G. Abstreiter, Phys. Rev. B **46**, 4071 (1992).
[12] R. Loudon, Adv. Phys. **13**, 423 (1964); W. Hayes and R. Loudon, *Scattering of Light by Crystals* (Wiley, New York, 1978), p. 169.
[13] G. Wei, J. Zi, K. Zhang, and X. Xie, J. Appl. Phys. **82**, 4693 (1997).
[14] F. Demangeot, J. Frandon, M. A. Renucci, B. Beaumont, and P. Gibart, in *Proceedings of the 9th Conference on Semiconducting and Insulating Materials*, edited by C. Fontaine (IEEE, Piscataway, N.J., 1996), p. 97.
[15] L. Landau and E. Lifchitz, *Quantum Mechanics* (Mir, Moscow, 1967), pp. 82–83.
[16] The m values given in Ref. 4 differ from our values, because we used another definition for the QC modes order in our work. This is why one $m=0$ QC mode (S or AS) was forbidden in Ref. 4 depending on the sign of $\epsilon_{z,1}(\omega)\epsilon_{z,2}(\omega)$, whereas we find S and AS modes for any positive m.
[17] M. V. Klein, IEEE J. Quantum Electron. **QE-22**, 1760 (1986).
[18] A. K. Sood, J. Menendez, M. Cardona, and K. Ploog, Phys. Rev. Lett. **54**, 2111 (1985).
[19] B. K. Ridley and M. Babiker, Phys. Rev. B **43**, 9096 (1991).
[20] B. Jusserand and M. Cardona, in *Light Scattering in Solids V*, edited by M. Cardona and G. Güntherodt (Springer, Heidelberg, 1989), pp. 75–76.
[21] V. Y. Davydov, N. S. Averkiev, I. N. Goncharuk, D. K. Nelson, I. Nikitina, A. S. Polkovnikov, A. N. Smirnov, M. A. Jacobson, and O. K. Semchinova, J. Appl. Phys. **82**, 5097 (1997).
[22] F. Demangeot, J. Frandon, M. A. Renucci, O. Briot, B. Gil, and R. L. Aulombard, Solid State Commun. **100**, 207 (1996).
[23] A. K. Sood, J. Menendez, M. Cardona, and K. Ploog, Phys. Rev. Lett. **54**, 2115 (1985).
[24] J. Gleize, F. Demangeot, J. Frandon, M. A. Renucci, F. Widmann, and B. Daudin, Appl. Phys. Lett. **74**, 703 (1999).
[25] V. Y. Davydov, Y. E. Kitaev, I. N. Goncharuk, A. N. Smirnov, J. Graul, O. Semchinova, D. Uffmann, M. B. Smirnov, A. P. Mirgorodsky, and R. A. Evarestov, Phys. Rev. B **58**, 12 899 (1998).
[26] L. E. McNeil, M. Grimsditch, and R. H. French, J. Am. Ceram. Soc. **76**, 1132 (1993).